



Development of a
high temporal–spatial
resolution vehicle
emission inventory –
Part 2

J. J. He et al.

Development of a high temporal–spatial resolution vehicle emission inventory based on NRT traffic data and its impact on air pollution in Beijing – Part 2: Impact of vehicle emission on urban air quality

J. J. He¹, L. Wu¹, H. J. Mao¹, H. L. Liu², B. Y. Jing¹, Y. Yu³, P. P. Ren¹, C. Feng⁴,
and X. H. Liu⁴

¹The College of Environmental Science & Engineering, Nankai University, Tianjin, China

²Chinese Academy of Meteorological Sciences, China Meteorological Administration, Beijing, China

³Clod & Arid Regions Environmental & Engineering Research Institute, Chinese Academy of Sciences, Lanzhou, China

⁴Tianjin Vehicle Emission Control Center, Tianjin, China

Title Page

Abstract

Introduction

Conclusions

References

Tables

Figures

◀

▶

◀

▶

Back

Close

Full Screen / Esc

Printer-friendly Version

Interactive Discussion



Received: 30 April 2015 – Accepted: 15 June 2015 – Published: 14 July 2015

Correspondence to: H. J. Mao (hongjun_mao@hotmail.com)
and H. L. Liu (liuhongli@cams.cma.gov.cn)

Published by Copernicus Publications on behalf of the European Geosciences Union.

ACPD

15, 19239–19273, 2015

**Development of a
high temporal–spatial
resolution vehicle
emission inventory –
Part 2**

J. J. He et al.

Title Page

Abstract

Introduction

Conclusions

References

Tables

Figures



Back

Close

Full Screen / Esc

Printer-friendly Version

Interactive Discussion



Abstract

In a companion paper (Jing et al., 2015), a high temporal–spatial resolution vehicle emission inventory (HTSVE) for 2013 in Beijing has been established based on near real time (NRT) traffic data and bottom up methodology. In this study, based on the sensitivity analysis method of switching on/off pollutant emissions in the Chinese air quality forecasting model CUACE, a modeling study was carried out to evaluate the contributions of vehicle emission to the air pollution in Beijing main urban areas in the periods of summer (July) and winter (December) 2013. Generally, CUACE model had good performance of pollutants concentration simulation. The model simulation has been improved by using HTSVE. The vehicle emission contribution (VEC) to ambient pollutant concentrations not only changes with seasons but also changes over moment. The mean VEC, affected by regional pollutant transports significantly, is 55.4 and 48.5 % for NO₂, while 5.4 and 10.5 % for PM_{2.5} in July and December 2013, respectively. Regardless of regional transports, relative vehicle emission contribution (RVEC) to NO₂ is 59.2 and 57.8 % in July and December 2013, while 8.7 and 13.9 % for PM_{2.5}. The RVEC to PM_{2.5} is lower than PM_{2.5} contribution rate for vehicle emission in total emission, which may be caused by easily dry deposition of PM_{2.5} from vehicle emission in near-surface layer compared to elevated source emission.

1 Introduction

In recent years, the serious atmospheric environment problems in China attract special attention from government, publics and researchers. Due to the control of coal combustion, the type of air pollution is changing from smoke to vehicle exhaust and mixed sources, and the secondary aerosols and regional transports play an important role in severe haze episodes (Zhang et al., 2006; Huang et al., 2014), which make it more difficult to control air pollution. Air pollution caused by traffic emission has become the main concern of pollution control, especially in metropolitan cities. Direct emission

Development of a high temporal–spatial resolution vehicle emission inventory – Part 2

J. J. He et al.

Title Page

Abstract

Introduction

Conclusions

References

Tables

Figures



Back

Close

Full Screen / Esc

Printer-friendly Version

Interactive Discussion



Development of a high temporal–spatial resolution vehicle emission inventory – Part 2

J. J. He et al.

Title Page

Abstract

Introduction

Conclusions

References

Tables

Figures

◀

▶

◀

▶

Back

Close

Full Screen / Esc

Printer-friendly Version

Interactive Discussion

pollutants from road traffic include nitrogen oxides (NO_x), carbon monoxide (CO), hydrocarbon (HC), particulate matter (PM) and so on (Zhou et al., 2005; Song and Xie, 2006). Based on RAINS-ASIA computer model, five sectors direct emissions of sulfur dioxide (SO_2), nitrogen oxides (NO_x) and carbon monoxide (CO) including industry, power, domestic, transportation and biofuels in 1990, 1995 and 2020 were estimated for China by Streets and Waldhoff (2000), the transportation sector contributed approximately 1 and 2 % to total SO_2 emissions, 9 and 12 % to total NO_x emissions, 14 and 22 % to total CO emissions in 1990 and 1995. Traffic emission has a significant contribution to urban air pollution in many cities in China (Qin and Chan, 1993; Fu et al., 2001), while more stringent vehicle emission standards lead to simultaneous reduction of surface ozone (O_3) and fine particulate matter ($\text{PM}_{2.5}$) concentrations (Saikawa et al., 2011).

Beijing, as the capital of China, is one of the most important metropolitan cities in the world, providing a habitat for a population over 21 million. The number of vehicle in Beijing increased rapidly during the last decades and hit 5.5 million in 2014, putting an immense pressure on environment. A lot of researches on the impact of vehicle emission in Beijing have completed from different perspective. Hao et al. (2001) developed vehicle emission inventory and investigated the contribution of traffic on atmospheric pollutant concentrations utilizing a Gaussian dispersion model in 1995, and vehicle emission contributed 76.8 and 40.2 % to total CO and NO_x emissions, 76.5 and 68.4 % to ambient CO and NO_x concentrations. During the Sino-African summit in 2006, the number concentrations of the particles and accumulation modes seemingly reduced by 20–60 % due to the strict traffic restrictions (Cheng et al., 2008). Zhang et al. (2011) evaluated the effectiveness of air pollution control through traffic restriction measure in August 2007 and discovered road mobile sources were more effective on dust elements than anthropogenic elements of PM. Based on positive matrix factorization (PMF), Liu et al. (2014) investigated the source apportionment of ambient fine particle and found the vehicle emission was mainly responsible for particles in the size range 10–50 nm and accounted for 47.9 % of particle number concentration during summertime in 2011.

**Development of a
high temporal–spatial
resolution vehicle
emission inventory –
Part 2**

J. J. He et al.

Title Page

Abstract

Introduction

Conclusions

References

Tables

Figures

◀

▶

◀

▶

Back

Close

Full Screen / Esc

Printer-friendly Version

Interactive Discussion



A series of emission control measurements and atmospheric observations during the 2008 Beijing Olympic Games created a valuable case to research the effectiveness of control measures on mitigating air pollution. It was illustrated that the black carbon (BC) concentration after traffic control during Olympic decreased 74 %, and diesel trucks were a major contribution to the ambient summertime BC levels (X. Wang et al., 2009). With the 32.3 % traffic flow reduction, numerical simulation revealed the average reduction rate of PM₁₀, CO, and NO₂ were 28, 19.3 and 12.3 % respectively, but an increase rate of O₃ was 25.2 % (Wang and Xie, 2009). Compared with uncontrolled period, on-road air pollutant concentrations during the Olympics air pollution control period, which is concluded from versatile mobile laboratory moving along Beijing's Fourth Ring Road, decreased significantly, by up to 54 % for CO, 41 % for NO_x, 70 % for SO₂ and 12 % for BC (M. Wang et al., 2009). Hence, there is a certain controversy between previous studies and a significant fluctuation of pollutant concentration contribution in different periods. Further researches should be conducted in traffic emission effect on Beijing's air quality resulted from air pollution and pollutants emission characteristics changes in recent years and later on.

In a companion paper (Jing et al., 2015), based on NRT traffic data, high temporal–spatial resolution vehicle emission inventory for 2013 in Beijing was established via a bottom up methodology. This part (Part 2) utilizes Chinese Unified Atmospheric Chemistry Environment (CUACE) model to simulate ambient pollutant concentrations and evaluate the contributions of vehicle emission in Beijing main urban areas in periods of summer and winter 2013 based on the sensitivity analysis method of switching on/off pollutant emissions. In Sect. 2, the details of the methods, datasets and model setup are shown. CUACE model evaluation and the effect of new vehicle emission inventory are presented in Sect. 3. The main conclusions are presented in Sect. 4.

2 Data and method

2.1 Model description

Developed by China Meteorological Administration (CMA), CUACE model is used to simulate air quality for Beijing in this study. CUACE model is a unified chemical weather numerical forecasting system which is independent with weather and climate model. It consists of four functional blocks: anthropogenic and natural emissions; atmospheric gaseous chemical mechanisms; atmospheric aerosol chemical mechanisms; numerical assimilation system. CUACE is applied to compute atmospheric chemical composition including black carbon (BC), organic carbon (OC), sulfate, nitrate, ammonia, dust, sea-salt and so on. CUACE is online coupled to fifth-generation Penn State/NCAR mesoscale model (MM5) and Global/Regional Assimilation and PreDiction System (GRAPSE), MM5 is selected to simulate mesoscale meteorological fields in this study. For different research target and application purpose, CUACE is designed with open interface to make it easily being integrated to different time and spatial scale models. A more detailed description can refer to Gong et al. (2009). The performance of CUACE was evaluated by many researchers. Wang et al. (2010) simulated dust weather occurred in April 2006 and indicated CUACE model could predict the outbreak, development, transport and depletion processes of sand and dust storms accurately over China and the East Asian region. Li et al. (2013) evaluated air quality prediction by CUACE model over Urumqi and acquired a quite accurate forecasting on air quality levels, especially for NO₂ and PM₁₀ levels. Given the good performance in air quality prediction, CUACE model has been used for haze forecasting in National Meteorological Center of CMA and some local environmental protection agencies.

2.2 Numerical simulation design

In this study, MM5-CUACE model is configured to have three nested domains to reduce spurious boundary effects in the inner domain with horizontal resolution of 27 km

Development of a high temporal–spatial resolution vehicle emission inventory – Part 2

J. J. He et al.

Title Page

Abstract

Introduction

Conclusions

References

Tables

Figures

◀

▶

◀

▶

Back

Close

Full Screen / Esc

Printer-friendly Version

Interactive Discussion



covering North China and the surrounding areas, 9 km covering Jing-Jin-Ji (Beijing, Tianjin and Hebei) areas and 3 km-resolution covering Beijing city and surrounding areas (Fig. 1). In the vertical, there are a total of 35 full eta levels extending to the model top at 10 hPa, with 16 levels below 2 km.

Two periods: July and December in 2013 are selected for model integration to evaluate different seasonal impact (summer and winter respectively) of vehicle emission on air quality. The time steps of MM5 and CUACE model are 15 and 150 s respectively. Driving field provides the initial, lateral and surface boundary conditions and transmits the weather background information to MM5. However, for large domain or long term simulations, the large-scale weather situation simulated by MM5 may diverge from that of the driving field. The methods to constrain MM5 to the driving field involve frequent re-initialization, analysis nudging, spectral nudging, and scale-selective bias correction (Bowden et al., 2013). 36 h re-initialization run is executed to simulate meteorological conditions and air quality, and the former 12 h simulation is discarded as spin up time, which is the same as Zhang et al. (2012). The initial and boundary meteorological conditions are from T639 reanalysis data with 30 km × 30 km spatial resolution and 6 h temporal resolution supplied by CMA (Xiao et al., 2010). The initial and boundary chemical conditions of the first simulation segment are based on averages from several field studies over eastern Pacific Ocean (McKeen et al., 2002), and other segment initial and boundary conditions are derived from previous simulation segment.

Two real simulations which based on default emission of CUACE and the improved emission with high temporal-spatial resolution vehicle emission (hereafter refer to HTSVE) are carried out to evaluate the accuracy of pollutant concentrations simulated by CUACE and analyze the influence of HTSVE on Beijing air quality, and hereafter refer to SIM1 and SIM2 respectively. In some studies, the zero out method was used to calculate contribution of various emission sources (Cheng et al., 2013). However, simulated pollutant concentration, which has a significant influence on contribution rate of emission sources, is anamorphic due to huge variability of ambient backward concentration. In this study, the vehicle emission contribution (VEC) to ambient pollutant

Development of a high temporal-spatial resolution vehicle emission inventory – Part 2

J. J. He et al.

[Title Page](#)[Abstract](#)[Introduction](#)[Conclusions](#)[References](#)[Tables](#)[Figures](#)[◀](#)[▶](#)[◀](#)[▶](#)[Back](#)[Close](#)[Full Screen / Esc](#)[Printer-friendly Version](#)[Interactive Discussion](#)

concentration is computed based on the sensitivity analysis method of switching on (SIM2) and off (here after refer to SIM3) vehicle emission in Beijing, and is shown as follows:

$$VEC = \frac{C_{SIM2} - C_{SIM3}}{C_{SIM2}} \times 100\% \quad (1)$$

where C represents pollutant concentration. In fact, the regional transports of pollutants has obviously effect on VEC, and we calculate relative vehicle emission contribution (RVEC) which does not consider pollutant regional transports, as shown in Eq. (2):

$$RVEC = \frac{C_{SIM2} - C_{SIM3}}{C_{SIM2} - C_{SIM4}} \times 100\% \quad (2)$$

where SIM4 represents the simulation of switching off all emission sources in Beijing. All simulation test schemes are listed in Table 1.

2.3 Emission inventory

CUACE model has an independent pollution emission module, which contains natural and anthropogenic emissions including many gas and particle matter emissions (Gong et al., 2009). Anthropogenic emissions of SO_2 , NO_x , CO, VOCs, $PM_{2.5}$, PM_{10} , BC, OC, etc. used in emission module were developed by CMA based on INTEX-B inventory, the emissions database for global atmospheric research (EDGAR) and environmental statistics database. Gridded INTEX-B inventory covers 22 countries and regions in East Asia with a resolution of $0.5^\circ \times 0.5^\circ$, and is classified into industry emission, power station emission, residential emission and vehicle emission (Zhang et al., 2009).

The EDGAR is a joint project of the European Commission Joint Research Centre and the Netherlands Environmental Assessment Agency. The environmental statistics database is supplied by Environmental Protection Agency. Finally emission inventory was pretreated by SMOKE for detailed temporal and spatial distribution. Hourly emissions were obtained for CUACE model input. The emission inventory is a key factor

Development of a high temporal–spatial resolution vehicle emission inventory – Part 2

J. J. He et al.

Title Page

Abstract

Introduction

Conclusions

References

Tables

Figures



Back

Close

Full Screen / Esc

Printer-friendly Version

Interactive Discussion



to air quality numerical simulation. Annual emissions of CO, NO_x, SO₂ and PM_{2.5} in CUACE model in Beijing are 3149.5, 173.8, 158.2 and 79.0 kt respectively. By comparing the different researches (Table 2) found that there are many uncertainties of inventories but it is difficult to identify which one is more accurate. As mentioned by Q. Z. Wu et al. (2014), the uncertainty is mostly derived from basic data, the method of establishing emission inventory, the emission factor and the date of basic data etc.

This study focus on vehicle source and its influence. HTSVE based on NRT traffic data was used to replace the vehicle emission in CUACE emission module to analyze its effects on air quality simulation. The detailed description of high temporal-spatial resolution vehicle emission and comparison with vehicle emission in CUACE emission module were presented in Part 1. The contribution of major species from vehicle emission is presented in Table 3. The vehicle emission of NO, NO₂ and HC from HTSVE is higher, while CO and PM_{2.5} is lower than that from CUACE.

2.4 Observational data

2.4.1 Meteorological data

The accuracy of mesoscale meteorological fields simulated by MM5 has a significant effect on air quality simulation, and it should be evaluated with observation data firstly. In this study, the observed near-surface meteorological fields including 2 m temperature, 2 m specific humidity and 10 m wind speed are obtained from Meteorological Information Comprehensive Analysis and Process System (MICAPS) of CMA. MICAPS surface data has eight conventional observation times everyday (00:00, 03:00, 06:00, 09:00, 12:00, 15:00, 18:00, 21:00 UTC) and 20 meteorological stations located in study region (Fig. 1a).

Development of a high temporal-spatial resolution vehicle emission inventory – Part 2

J. J. He et al.

Title Page

Abstract

Introduction

Conclusions

References

Tables

Figures

◀

▶

◀

▶

Back

Close

Full Screen / Esc

Printer-friendly Version

Interactive Discussion



2.4.2 Air quality data

To evaluate simulated air quality by CUACE, hourly near-surface average concentrations of NO_2 and $\text{PM}_{2.5}$ from 9 atmospheric environment monitoring stations in Beijing (shown in Fig. 1b) in simulation periods were acquired from China National Environment Monitoring Centre. The monitoring stations distributed in study region could reflect different area pollution level and capture overall air quality in Beijing city.

3 Results and discussions

3.1 Model evaluation and the impact of new vehicle emission inventory

The accuracy of air quality simulation based on numerical model greatly relates to mesoscale meteorological simulation. Although the good performance of MM5 has obtained in many studies, the MM5's results is verified firstly as the different accuracy of meteorological fields in different study domains, seasons and physical parameterizations. Based on statistical analysis, 2 m temperature root mean square error (RMSE) and correlation coefficient (R) are 3.4 K and 0.81 in July, 3.8 K and 0.87 in December. MM5 can capture temporal and spatial variation of near-surface temperature effectively. 2 m specific humidity RMSE and R are 2.4 g kg^{-1} and 0.56 in July, 0.9 g kg^{-1} and 0.82 in December, which indicates that basic temporal and spatial variation of near-surface specific humidity is simulated by MM5. 10 m wind speed RMSE and R are 1.4 ms^{-1} and 0.37 in July, 1.7 ms^{-1} and 0.57 in December. The RMSE was 1–4 K for 2 m temperature, 1–2 g kg^{-1} for 2 m specific humidity and 1–4 ms^{-1} for 10 m wind speed in most studies (Han et al., 2008; Jiménez-Guerrero et al., 2008; Papalexidou and Mousiopoulos, 2006; Miao et al., 2008). In this study, MM5 presents the essential features of the local circulation over Beijing as seen from above analysis and its performance observed here is comparable to other studies generally.

Development of a high temporal–spatial resolution vehicle emission inventory – Part 2

J. J. He et al.

Title Page

Abstract

Introduction

Conclusions

References

Tables

Figures

◀

▶

◀

▶

Back

Close

Full Screen / Esc

Printer-friendly Version

Interactive Discussion



NO₂ and PM_{2.5} are the major concerns as they are susceptible to vehicle emission. Interval of simulated and observed daily mean near-surface NO₂ and PM_{2.5} concentrations averaged over 9 sites during two periods are shown in Fig. 2. CUACE model underestimates the NO₂ concentration significantly, especially during serious pollution periods. Due to the increasing emission of HTSVE (Table 2), the NO₂ concentration from SIM2 increases 31.8 and 11.1 % in July and December respectively, resulting in significant improvement to the previous underestimates. The RMSEs of NO₂ daily mean concentration decrease 17.6 and 10.9 % in two periods when HTSVE is used. Temporal correlation coefficients of NO₂ daily mean concentrations for SIM1 and SIM2 are 0.80 and 0.79 respectively in December, which indicates CAUCE can reproduce NO₂ time trends accurately. However, low correlation (0.21 and 0.12 for SIM1 and SIM2 respectively) in July reflects the complexity of air quality numerical simulation. Simulated PM_{2.5} daily mean concentration is basically consistent with observed value. Minor difference of PM_{2.5} concentration is observed between SIM1 and SIM2 due to less vehicle emission change (Table 3). Based on temporal correlation analysis, SIM2 improves PM_{2.5} time trends slightly, with correlation coefficients of 0.75 and 0.77 in two periods for SIM1, 0.76 and 0.78 for SIM2. Compared with SIM1, the RMSE of PM_{2.5} daily mean concentration has slightly decrease for SIM2. It is obviously that simulated PM_{2.5} concentration is more accurate than simulated NO₂ concentration in July. CUACE's ability is evaluated through the comparison of model grid and site station values, however, this method has several uncertainties because the local information is involved. It should be noted that the lifetime of ambient NO₂ is shorter than that of ambient PM_{2.5}, and local characteristics are more significantly for NO₂. This may be one of the reason for the poor performance of NO₂ simulation. Seasonal difference of CUACE model performance is also found in this study, with accurately simulation in winter, and this may relate to meteorological condition, especially on wind field bias as mentioned above. Overall, the performance of CUACE model is comparable with other studies in Beijing (Gao et al., 2011; Wu et al., 2011). As better performance acquired by SIM2, it is made as a baseline scenario in the flowing analysis.

Development of a high temporal–spatial resolution vehicle emission inventory – Part 2

J. J. He et al.

Title Page

Abstract

Introduction

Conclusions

References

Tables

Figures

◀

▶

◀

▶

Back

Close

Full Screen / Esc

Printer-friendly Version

Interactive Discussion



Spatial distribution of pollutant concentration relates to pollutant emission distribution and meteorological condition. The mean wind in Beijing urban region is the southwest wind in July, and drives local pollutant transports from southwest to northeast. The high NO₂ concentration is located in northeastern city, while two high PM_{2.5} concentration regions appear in west and center city (Fig. 3a and b). The spatial distribution of NO₂ is different from that of PM_{2.5} because of emission sources distribution difference. The mean concentrations of NO₂ and PM_{2.5} are 29.8 and 91.3 μg m⁻³ in July. Beijing urban region is dominated by northwest wind in December, and pollutant concentration distribution is obviously different from that in July. NO₂ concentration is high in southeast city, and gradually decreases outward (Fig. 3c). High PM_{2.5} concentration is mostly located in west and southeast city (Fig. 3d). It is found that significant difference presents in NO₂ distribution between July and December while slightly difference for PM_{2.5}. The mean concentrations of NO₂ and PM_{2.5} are 42.8 and 136.4 μg m⁻³ in December respectively.

3.2 The effect of vehicle emission on urban air quality

VEC on ambient pollutant concentration is analyzed through comparison simulation with and without vehicle emission (SIM2 and SIM3 respectively). Probability density function (PDF) is a good way to describe the total representation. The PDF of instantaneous VEC in two periods is shown in Fig. 4. The maximum frequencies of VEC to NO₂ in July and December are appeared in 55–60 and 50–55 % respectively. The frequencies of VEC to NO₂ from 15 to 60 % in December are larger than that in July (Fig. 4a), which indicates large contribution presents in summer while small contribution presents in winter. This may relates to seasonal differences of meteorological condition and pollutant emission. In summer, high temperature and strong solar radiation lead to strong atmosphere oxidation ability, and therefore it is easy to convert from NO to NO₂, which results in large contribution to NO₂ concentration. Meanwhile, the high rate of NO₂ emission from vehicle (Table 3) is another reason for large contribution to ambient NO₂

concentration in summer. The VEC to $\text{PM}_{2.5}$ is considerably lower than that to NO_2 . The maximum frequencies of VEC to $\text{PM}_{2.5}$ in July and December are appeared in 0–5 and 5–10 % respectively. Different from NO_2 , the mean VEC to $\text{PM}_{2.5}$ in summer is smaller than that in winter. Relative humidity in summer is larger than that in winter, and high relative humidity is conducive to gas-particle conversion processes of other emission sources (Yao et al., 2014), which may be one of the reason for small VEC to $\text{PM}_{2.5}$ in summer. Wind field variation is another reason for seasonal change of VEC to $\text{PM}_{2.5}$, which will be investigated in the following part.

As the local transports of pollutants, the VEC in Beijing city depends on wind field and spatial distribution of vehicle emission. Wind dependency map of VEC to NO_2 and $\text{PM}_{2.5}$ are shown in Fig. 5. High VEC to NO_2 in July is appeared in south wind with 3–4 ms^{-1} , while north wind with 6–7 ms^{-1} for that in December. Due to the difference of lifetime between NO_2 and $\text{PM}_{2.5}$, the wind dependency map to $\text{PM}_{2.5}$ is quite different from that to NO_2 . High VEC to $\text{PM}_{2.5}$ in July and December appeared in north wind due to many vehicle emission of particle matter in northeast city (Jing et al., 2015). The dominant wind is southwest wind in July and northwest in December (Fig. 3), which brings a small VEC to $\text{PM}_{2.5}$ in summer.

Figure 6 shows time series of VEC to NO_2 and $\text{PM}_{2.5}$ daily mean concentrations in main urban areas (within the 6th ring road) in two periods. The VEC not only changes with seasons, which is consistent with Cheng et al. (2007), but also changes with time. Time series of regional mean VEC is 49.8–60.0 % to ambient NO_2 concentration in July, with a mean contribution rate of 55.4 %. In December, regional mean contribution on NO_2 concentration decreases to 28.5–57.9 % at different days, with a mean contribution rate of 48.5 %. VEC to ambient $\text{PM}_{2.5}$ concentration is less than 10.3 and 13.6 % at different times, with mean contribution rate of 5.4 and 10.5 % in July and December respectively. The change of VEC to $\text{PM}_{2.5}$ between July and December is most caused by meteorological condition in two periods. With different lift time of $\text{PM}_{2.5}$ and NO_2 , $\text{PM}_{2.5}$ concentration is more affected by regional transports, while NO_2 concentration is more affected by local emissions. Therefore the contribution with time variation for

Development of a high temporal–spatial resolution vehicle emission inventory – Part 2

J. J. He et al.

Title Page

Abstract

Introduction

Conclusions

References

Tables

Figures

◀

▶

◀

▶

Back

Close

Full Screen / Esc

Printer-friendly Version

Interactive Discussion



PM_{2.5} is different from that for NO₂. Except for wind field, pollution level is an important factor to VEC. It is obviously that low VEC presents in serious pollution, while high VEC presents in low pollution concentration level, especially for NO₂ (Fig. 7).

The VEC has a significant spatial variation, previous study pointed that PM_{2.5} had larger contribution from vehicle emission (13.0–16.3 % vs. 5.1 %) in urban as compared to that in suburban (S. W. Wu et al., 2014). Figure 8 shows the spatial distribution of mean contribution rate of vehicle emission in two periods. Vehicle emission contributes 26.0–76.4 and 22.9–66.4 % of NO₂ at different regions in July and December. Significant effect of vehicle emission on ambient NO₂ concentration level is found in southeast and northeast city. VEC to PM_{2.5} is 1.2–15.4 and 2.4–24.4 % in July and December. The large contribution appears in northeast city in both summer and winter, which is widely different from the distribution of NO₂ contribution.

As can be seen from Table 4, receptor source apportionment and numerical sensitivity analysis are two main methods to compute VEC on ambient pollutant concentration, and VEC has significantly uncertainties from previous studies. In summary, vehicle emission contributes 4–17 and 22 % to PM_{2.5} concentration based on receptor source apportionment and numerical simulation methods, and 56–74 % to NO_x concentration based on numerical simulation method. The difference of the vehicle emission contribution to PM_{2.5} with the different methods is relatively large. The uncertainties of VEC are related to sampling or simulation time, the location, analysis method and weather conditions. The results from receptor source apportionment (CMB, PMF etc.) only represent the characteristics of receptor point and can be applied for primary pollutants (Cheng et al., 2015), however it is different from numerical sensitivity analysis which normally describes the regional characteristics and applies for primary and secondary pollutants. The uncertainty of emission source in numerical model may be the main reason for significant difference to VEC in previous numerical studies. Though relatively short simulation in this study, our results are comparable with previous studies, and meanwhile keep the difference which comes from analyzing periods and method.

Development of a high temporal–spatial resolution vehicle emission inventory – Part 2

J. J. He et al.

Title Page

Abstract

Introduction

Conclusions

References

Tables

Figures

◀

▶

◀

▶

Back

Close

Full Screen / Esc

Printer-friendly Version

Interactive Discussion



In this study, the rates of NO₂ and PM_{2.5} from vehicle emission in total emission takes account for 55.1 and 22.3 % in July and 53.9 and 20.6 % in December (Table 3) of total emission. Because of the effect of pollutant regional transports, the contribution rate of vehicle emission on ambient pollutant concentration is lower than the rate of vehicle emission in total emissions. The difference between these two rates became significantly larger with more contribution of outside emission, which implies the importance of weather condition. In order to avoid the effect of weather situation on analysis results, the relative contribution of vehicle emission on pollutant concentrations is analyzed in following section.

3.3 Relative contribution of vehicle emission

Air pollution in Beijing is attributed not only from local emissions but also from regional transports. Using the CMAQ model, An et al. (2007) investigated the contribution to pollutant concentrations in Beijing by using emission switch on/off method, the contribution of non-local emission accounted for 15–53 % of PM_{2.5}. Wu et al. (2011) studied the contribution to air pollution during CAREBeijing-2006, and local emission in Beijing accounted for 65 % of SO₂, 75 % of PM₁₀ and 90 % of NO₂ concentrations. Pollutant regional transport depends on atmospheric circulation and regional emission characteristics. By comparing pollutant concentrations between SIM2 and SIM4, local emissions in Beijing contributes 93.6 and 62.6 % to NO₂ and PM_{2.5} concentrations in July, and 83.8 and 76.1 % to NO₂ and PM_{2.5} concentrations in December, which have a profound effect on RVEC.

Figure 9 depicts the spatial distribution of RVEC to NO₂ and PM_{2.5} in July and December, and similar distribution is found in two periods. The RVEC to NO₂ is large in southeast and northeast main urban areas, while small in west main urban areas. Time series of regional mean RVEC to NO₂ in main urban areas range from 52.3 to 63.4 %, and 49.4 to 61.2 %, with the mean of 59.2 and 57.8 % in July and December respectively. Different from NO₂, the RVEC to PM_{2.5} is large in northeast of main urban areas in two periods. Time series of regional mean RVEC to PM_{2.5} range from 5.7 to 11.3 %

Development of a high temporal–spatial resolution vehicle emission inventory – Part 2

J. J. He et al.

Title Page

Abstract

Introduction

Conclusions

References

Tables

Figures

◀

▶

◀

▶

Back

Close

Full Screen / Esc

Printer-friendly Version

Interactive Discussion



Development of a high temporal–spatial resolution vehicle emission inventory – Part 2

J. J. He et al.

Title Page

Abstract

Introduction

Conclusions

References

Tables

Figures

◀

▶

◀

▶

Back

Close

Full Screen / Esc

Printer-friendly Version

Interactive Discussion

and 9.9 to 16.1 %, with the mean of 8.7 and 13.9 % in July and December respectively. High $PM_{2.5}$ emission from vehicle is found between north Fourth Ring Road and north Five Ring Road (see Part 1, Fig. 9). Controlled by southwest wind, $PM_{2.5}$ from vehicle is easily transferred out of the main urban areas, which results in low RVEC in July. However, the most of $PM_{2.5}$ from vehicle stay in east main city controlled by northwest wind, which results in high RVEC in December. Based on zero out method which did not involve regional transports, Cheng et al. (2013) found the contribution rates to pollutant concentrations were higher than those to the emissions because near-surface emission from vehicle facilitated greater contribution to local pollutant concentrations on the ground level. Regardless of regional transports, the contribution of vehicle emission to ambient $PM_{2.5}$ concentration is substantial lower than the rate of vehicle emission in total emission in this study. Our finding is seemingly in conflict with Cheng et al. (2013), but may be more reasonable for following two reasons. Different from elevated emission, $PM_{2.5}$ from vehicle emission in near-surface layer easily descends to the ground or is absorbed by vegetation, which leads to low contribution rate to $PM_{2.5}$ concentration. Furthermore, the zero out method is anamorphic because it obviously changes background concentrations and chemical processes in atmosphere.

4 Conclusion

Air quality simulation has been improved by using HTSVE. In summer (July), high NO_2 concentration was located in the northeastern part of city, while two high $PM_{2.5}$ concentration regions appeared in west and center of the city. In winter (December), NO_2 concentration was high in southeast city, then gradually decreased outward, while high $PM_{2.5}$ concentration was mostly located in west and southeast part of city. The VEC in Beijing city depends on wind field, spatial distribution of vehicle emission and air pollution level. High VEC to NO_2 in July appeared along with south wind and low pollution concentration level, while north wind and low pollution concentration level for that in

December. High VEC to PM_{2.5} in July and December appeared along with north wind and low pollution concentration level.

Seasonal change of VEC was observed in this study. The mean VECs to NO₂ were 55.4 and 48.5%, while the mean VECs to PM_{2.5} were 5.4 and 10.5% in July and December respectively. Regional pollutants transport was one of the most important reason for small contribution rate for ambient pollutant concentrations compared with contribution rate for pollutant emission in Beijing. Sensitivity analysis indicated that all local emissions in Beijing contributed 93.6 and 62.6% to NO₂ and PM_{2.5} concentrations in July, and 83.8 and 76.1% to NO₂ and PM_{2.5} concentrations in December, which had an important effect on RVEC. Regardless of regional transports, the RVEC to NO₂ was large in the southeast and northeast main urban areas, and northeast main urban areas for PM_{2.5}. The mean RVECs to NO₂ were 59.2 and 57.8%, while the mean RVECs to PM_{2.5} were 8.7 and 13.9% in July and December respectively. The RVEC to PM_{2.5} was lower than PM_{2.5} contribution rate for vehicle emission, which was caused by easily dry deposition of PM_{2.5} from vehicle emission in near-surface layer.

Acknowledgements. This work was supported by Chnia's National 863 program (2012AA063303) and the National Science and Technology Infrastructure Program (2014BAC16B03). The contents of this paper are solely the responsibility of the authors and do not necessarily represent official views of the sponsors.

References

- An, X., Zhu, T., Wang, Z., Li, C., and Wang, Y.: A modeling analysis of a heavy air pollution episode occurred in Beijing, *Atmos. Chem. Phys.*, 7, 3103–3114, doi:10.5194/acp-7-3103-2007, 2007.
- Bowden, J. H., Nolte, C. G., and Otte, T. L.: Simulating the impact of the large-scale circulation on the 2 m temperature and precipitation climatology, *Clim. Dynam.*, 40, 1903–1920, doi:10.1007/s00382-012-1440-y, 2013.

Development of a high temporal–spatial resolution vehicle emission inventory – Part 2

J. J. He et al.

Title Page

Abstract

Introduction

Conclusions

References

Tables

Figures

◀

▶

◀

▶

Back

Close

Full Screen / Esc

Printer-friendly Version

Interactive Discussion



**Development of a
high temporal–spatial
resolution vehicle
emission inventory –
Part 2**

J. J. He et al.

Title Page

Abstract

Introduction

Conclusions

References

Tables

Figures

◀

▶

◀

▶

Back

Close

Full Screen / Esc

Printer-friendly Version

Interactive Discussion



- Cao, G. L., Zhang, X. Y., Gong, S. L., An, X. Q., and Wang, Y. Q.: Emission inventories of primary particles and pollutant gases for China, *Chinese Sci. Bull.*, 56, 781–788, doi:10.1007/s11434-011-4373-7, 2011.
- Cheng, I., Xu, X., and Zhang, L.: Overview of receptor-based source apportionment studies for speciated atmospheric mercury, *Atmos. Chem. Phys. Discuss.*, 15, 5493–5536, doi:10.5194/acpd-15-5493-2015, 2015.
- Cheng, S. Y., Chen, D. S., Li, J. B., Wang, H. Y., and Guo, X. R.: The assessment of emission-source contributions to air quality by using a coupled MM5-ARPS-CMAQ modeling system: a case study in the Beijing metropolitan region, China, *Environ. Modell. Softw.*, 22, 1601–1616, doi:10.1016/j.envsoft.2006.11.003, 2007.
- Cheng, S. Y., Lang, J. L., Zhou, Y., Han, L. H., Wang, G., and Chen, D. S.: A new monitoring-simulation-source apportionment approach for investigating the vehicular emission contribution to the PM_{2.5} pollution in Beijing, China, *Atmos. Environ.*, 79, 308–316, doi:10.1016/j.atmosenv.2013.06.043, 2013.
- Cheng, Y. F., Heintzenberg, J., Wehner, B., Wu, Z. J., Su, H., Hu, M., and Mao, J. T.: Traffic restrictions in Beijing during the Sino-African Summit 2006: aerosol size distribution and visibility compared to long-term in situ observations, *Atmos. Chem. Phys.*, 8, 7583–7594, doi:10.5194/acp-8-7583-2008, 2008.
- Fu, L. X., Hao, J. M., He, D. Q., and He, K. B.: Assessment of vehicle pollution in China, *J. Air. Waste Manage.*, 51, 658–668, 2001.
- Gao, Y., Liu, X., Zhao, C., and Zhang, M.: Emission controls versus meteorological conditions in determining aerosol concentrations in Beijing during the 2008 Olympic Games, *Atmos. Chem. Phys.*, 11, 12437–12451, doi:10.5194/acp-11-12437-2011, 2011.
- Gong, S. L., Zhang, X. Y., Zhou, C. H., Liu, H. L., An, X. Q., Niu, T., Xue, M., Cao, G. L., and Cheng, Y. L.: Chemical weather forecasting system CUACE and application in China's regional haze forecasting, in: *Proceeding of the 26th Annual Meeting of Chinese Meteorological Society*, Hangzhou, 2009.
- Han, Z. W., Ueda, H., and An, J. L.: Evaluation and intercomparison of meteorological predictions by five MM5-PBL parameterizations in combination with three land-surface models, *Atmos. Environ.*, 42, 233–249, doi:10.1016/j.atmosenv.2007.09.053, 2008.
- Hao, J. M., Wu, Y., Fu, L. X., He, K. B., and He, D. Q.: Motor vehicle source contributions to air pollutants in Beijing, *Environ. Sci.*, 22, 1–6, 2001.

Development of a high temporal–spatial resolution vehicle emission inventory – Part 2

J. J. He et al.

Title Page

Abstract

Introduction

Conclusions

References

Tables

Figures

◀

▶

◀

▶

Back

Close

Full Screen / Esc

Printer-friendly Version

Interactive Discussion

- Hao, J. M., Wang, L. T., Li, L., Hu, J. N., and Yu, X. C.: Air pollutants contribution and control strategies of energy-use related sources in Beijing, *Sci. China Ser. D*, 48, 138–146, 2005.
- Huang, R. J., Zhang, Y. L., Bozzetti, C., Ho, K. F., Cao, J. J., Han, Y. M., Daellenbach, K. R., Slowik, J. G., Platt, S. M., Canonaco, F., Zotter, P., Wolf, R., Pieber, S. M., Bruns, E. A., Crippa, M., Ciarelli, G., Piazzalunga, A., Schwikowski, M., Abbaszade, G., Schnelle-Kreis, J., Zimmermann, R., An, Z. S., Szidat, S., Baltensperger, U., Haddad, I. E., and Prévôt, A. S. H.: High secondary aerosol contribution to particulate pollution during haze events in China, *Nature*, 514, 218–222, doi:10.1038/nature13774, 2014.
- Jiménez-Guerrero, P., Jorba, O., Baldasano, J. M., and Gassó, S.: The use of a modeling system as a tool for air quality management: annual high-resolution simulation and evaluation, *Sci. Total Environ.*, 390, 323–340, doi:10.1016/j.scitotenv.2007.10.025, 2008.
- Jing, B. Y., Wu, L., Mao, H. J., Gong, S. L., He, J. J., Zou, C., Song, G. H., and Li, X. Y.: Development of a high temporal–spatial resolution vehicle emission inventory based on NRT traffic data and its impact on air pollution in Beijing – Part 1: Development and evaluation of vehicle emission inventory, *Atmos. Chem. Phys. Discuss.*, in review, 2015.
- Li, M., Zhang, Z. Y., Liu, S. J., Yu, X. J., and Ju, C. X.: Verification of CUACE air quality forecast in Urumqi, *Desert Oasis Meteorol.*, 8, 63–68, 2014.
- Liu, Z. R., Hu, B., Liu, Q., Sun, Y., and Wang, Y. S.: Source apportionment of urban fine particle number concentration during summertime in Beijing, *Atmos. Environ.*, 96, 359–369, 2014.
- McKeen, S. A., Wotawa, G., Parrish, D. D., Holloway, J. S., Buhr, M. P., Hubler, G., Fehsenfeld, F. C., and Meagher, J. F.: Ozone production from Canadian wildfires during June and July of 1995, *J. Geophys. Res.*, 107, 4192, doi:10.1029/2001JD000697, 2002.
- Miao, S. G., Chen, F., Lemone, M. A., Tewari, M., Li, Q. C., and Wang, Y. C.: An observational and modeling study of characteristics of urban heat island and boundary layer structures in Beijing, *J. Appl. Meteorol. Clim.*, 48, 484–501, doi:10.1175/2008JAMC1909.1, 2008.
- Papalexiou, S. and Moussiopoulos, N.: Wind flow and photochemical air pollution in Thessaloniki, Greece. Part II: Statistical evaluation of European Zooming Model's simulation results, *Environ. Modell. Softw.*, 21, 1752–1758, doi:10.1016/j.envsoft.2005.09.004, 2006.
- Qin, Y. and Chan, L. Y.: Traffic source emission and street level air pollution in urban areas of Guangzhou, South China (P.R.C.), *Atmos. Environ.*, 27B, 275–282, 1993.
- Saikawa, E., Kurokawa, J., Takigawa, M., Borken-Kleefeld, J., Mauzerall, D. L., Horowitz, L. W., and Ohara, T.: The impact of China's vehicle emissions on regional air quality in 2000 and

**Development of a
high temporal–spatial
resolution vehicle
emission inventory –
Part 2**

J. J. He et al.

Title Page

Abstract

Introduction

Conclusions

References

Tables

Figures

◀

▶

◀

▶

Back

Close

Full Screen / Esc

Printer-friendly Version

Interactive Discussion



2020: a scenario analysis, *Atmos. Chem. Phys.*, 11, 9465–9484, doi:10.5194/acp-11-9465-2011, 2011.

Song, X. Y. and Xie, S. D.: Development of vehicle emission inventory in China, *Environ. Sci.*, 27, 1041–1045, 2006.

5 Song, Y., Xie, S. D., Zhang, Y. H., Zeng, L. M., Salmon, L. G., and Zheng, M.: Source apportionment of PM_{2.5} in Beijing using principal component analysis/absolute principal component scores and UNMIX, *Sci. Total Environ.*, 372, 278–286, doi:10.1016/j.scitotenv.2006.08.041, 2006.

Streets, D. G. and Waldhoff, S. T.: Present and future emissions of air pollutants in China: SO₂, NO_x, and CO, *Atmos. Environ.*, 34, 363–374, doi:10.1016/S1352-2310(99)00167-3, 2000.

10 Wang, H. L., Zhuang, Y. H., Wang, Y., Sun, Y., Yuan, H., Zhuang, G. S., and Hao, Z. P.: Long-term monitoring and source apportionment of PM_{2.5}/PM₁₀ in Beijing, China, *J. Environ. Sci.*, 20, 1323–1327, doi:10.1016/S1001-0742(08)62228-7, 2008.

15 Wang, H., Gong, S. L., Zhang, H. L., Chen, Y., Shen, X. S., Chen, D. H., Xue, J. S., Shen, Y. F., Wu, X. J., and Jin, Z. Y.: A new-generation sand and dust storm forecasting system GRAPES_CUACE/Dust: model development, verification and numerical simulation, *Chinese Sci. Bull.*, 55, 635–649, 2010.

20 Wang, M., Zhu, T., Zheng, J., Zhang, R. Y., Zhang, S. Q., Xie, X. X., Han, Y. Q., and Li, Y.: Use of a mobile laboratory to evaluate changes in on-road air pollutants during the Beijing 2008 Summer Olympics, *Atmos. Chem. Phys.*, 9, 8247–8263, doi:10.5194/acp-9-8247-2009, 2009.

Wang, T. and Xie, S.: Assessment of traffic-related air pollution in the urban streets before and during the 2008 Beijing Olympic Games traffic control period, *Atmos. Environ.*, 43, 5682–5690, doi:10.1016/j.atmosenv.2009.07.034, 2009.

25 Wang, X., Westerdahl, D., Chen, L. C., Wu, Y., Hao, J. M., Pan, X. C., Guo, X. B., and Zhang, K. M.: Evaluating the air quality impacts of 2008 Beijing Olympic Games: on-road emission factors and black carbon profiles, *Atmos. Environ.*, 43, 4535–4543, doi:10.1016/j.atmosenv.2009.06.054, 2009.

30 Wu, Q. Z., Wang, Z. F., Gbaguidi, A., Gao, C., Li, L. N., and Wang, W.: A numerical study of contributions to air pollution in Beijing during CAREBeijing-2006, *Atmos. Chem. Phys.*, 11, 5997–6011, doi:10.5194/acp-11-5997-2011, 2011.

Wu, Q. Z., Xu, W. S., Shi, A. J., Li, Y. T., Zhao, X. J., Wang, Z. F., Li, J. X., and Wang, L. N.: Air quality forecast of PM₁₀ in Beijing with Community Multi-scale Air Quality Modeling (CMAQ)

system: emission and improvement, *Geosci. Model Dev.*, 7, 2243–2259, doi:10.5194/gmd-7-2243-2014, 2014.

Wu, S. W., Deng, F. R., Wei, H. Y., Huang, J., Wang, X., Hao, Y., Zheng, C. J., Qin, Y., Lv, H. B., Shima, M., and Guo, X. B.: Association of cardiopulmonary health effects with source-appointed ambient fine particulate in Beijing, China: a combined analysis from the healthy volunteer natural relocation (HVNR) study, *Environ. Sci. Technol.*, 48, 3438–3448, doi:10.1021/es404778w, 2014.

Xiao, D., Deng, L. T., Chen, J., and Hu, J. K.: Tentative verification and comparison of WRF forecasts driven by data from T213 and T639 models, *Torrent. Rain Disast.*, 29, 20–29, 2010.

Yao, Q., Cai, Z. Y., Han, S. Q., Liu, A. X., and Liu, J. L.: Effects of relative humidity on the aerosol size distribution and visibility in the winter in Tianjin, China *Environ. Sci.*, 34, 596–603, 2014.

Yu, L. D., Wang, G. F., Zhang, R. J., Zhang, L. M., Song, Y., Wu, B. B., Li, X. F., An, K., and Chu, J. H.: Characterization and source apportionment of PM_{2.5} in an urban environment in Beijing, *Aerosol Air Qual. Res.*, 13, 574–583, doi:10.4209/aaqr.2012.07.0192, 2013.

Zhang, J. P., Zhu, T., Zhang, Q. H., Li, C. C., Shu, H. L., Ying, Y., Dai, Z. P., Wang, X., Liu, X. Y., Liang, A. M., Shen, H. X., and Yi, B. Q.: The impact of circulation patterns on regional transport pathways and air quality over Beijing and its surroundings, *Atmos. Chem. Phys.*, 12, 5031–5053, doi:10.5194/acp-12-5031-2012, 2012.

Zhang, M. G., Pu, Y., Zhang, R., and Han, Z.: Simulation of sulfur transport and transformation in East Asia with a comprehensive chemical transport model, *Environ. Modell. Softw.*, 21, 812–820, 2006.

Zhang, Q., Streets, D. G., Carmichael, G. R., He, K. B., Huo, H., Kannari, A., Klimont, Z., Park, I. S., Reddy, S., Fu, J. S., Chen, D., Duan, L., Lei, Y., Wang, L. T., and Yao, Z. L.: Asian emissions in 2006 for the NASA INTEX-B mission, *Atmos. Chem. Phys.*, 9, 5131–5153, doi:10.5194/acp-9-5131-2009, 2009.

Zhang, R. J., Shen, Z. X., Zhang, L. M., Zhang, M. G., Wang, X., and Zhang, K.: Element composition of particles during periods with and without traffic restriction in Beijing: the effectiveness of traffic restriction measure, *Scient. Onl. Lett. Atmos.*, 7, 61–64, doi:10.2151/sola.2011-016, 2011.

Zhang, R., Jing, J., Tao, J., Hsu, S.-C., Wang, G., Cao, J., Lee, C. S. L., Zhu, L., Chen, Z., Zhao, Y., and Shen, Z.: Chemical characterization and source apportionment of PM_{2.5} in Beijing: seasonal perspective, *Atmos. Chem. Phys.*, 13, 7053–7074, doi:10.5194/acp-13-7053-2013, 2013.

Development of a high temporal–spatial resolution vehicle emission inventory – Part 2

J. J. He et al.

Title Page

Abstract

Introduction

Conclusions

References

Tables

Figures



Back

Close

Full Screen / Esc

Printer-friendly Version

Interactive Discussion



**Development of a
high temporal–spatial
resolution vehicle
emission inventory –
Part 2**

J. J. He et al.

Title Page

Abstract

Introduction

Conclusions

References

Tables

Figures

◀

▶

◀

▶

Back

Close

Full Screen / Esc

Printer-friendly Version

Interactive Discussion

- Zhao, B., Wang, P., Ma, J. Z., Zhu, S., Pozzer, A., and Li, W.: A high-resolution emission inventory of primary pollutants for the Huabei region, China, *Atmos. Chem. Phys.*, 12, 481–501, doi:10.5194/acp-12-481-2012, 2012.
- 5 Zheng, M., Salmon, L. G., Schauer, J. J., Zeng, L. M., Kiang, C. S., Zhang, Y. H., and Cass, G. R.: Seasonal trends in $PM_{2.5}$ source contributions in Beijing, China, *Atmos. Environ.*, 39, 3967–3976, doi:10.1016/j.atmosenv.2005.03.036, 2005.
- Zhou, Y., Fu, L. X., Yang, W. S., and Wang, Y.: Analysis of vehicle emission in Beijing by remote sensing monitoring, *Tech. Equip. Environ. Poll. Contr.*, 6, 91–94, 2005.

Development of a high temporal–spatial resolution vehicle emission inventory – Part 2

J. J. He et al.

Title Page

Abstract

Introduction

Conclusions

References

Tables

Figures

◀

▶

◀

▶

Back

Close

Full Screen / Esc

Printer-friendly Version

Interactive Discussion

Table 1. Numerical simulation schemes.

Numerical simulation	Emission source
SIM1	Default emission of CUACE
SIM2	Improved emission with Beijing HTSVE
SIM3	Switch off Beijing vehicle emission
SIM4	Switch off Beijing anthropogenic emission

Development of a high temporal–spatial resolution vehicle emission inventory – Part 2

J. J. He et al.

Table 2. Emission of major anthropogenic species in Beijing (unit: 10^3 tyr^{-1}).

Source	CO	NO _x	SO ₂	PM _{2.5}
CUACE emission	3149.5	173.8	158.2	79.0
An et al. (2007)	1021.8	227.0	211.3	53.4
Zhang et al. (2009)	2591.0	327.0	248.0	90.0
Cao et al. (2011)	1998.0	437.0	172.0	162.0
Wu et al. (2011)		236.2	172.5	67.9
Zhao et al. (2012)	2580.0	309.0	187.0	90.0
Q. Z. Wu et al. (2014)	1793.8	200.0	78.8	59.1

Title Page

Abstract

Introduction

Conclusions

References

Tables

Figures

◀

▶

◀

▶

Back

Close

Full Screen / Esc

Printer-friendly Version

Interactive Discussion

Development of a high temporal–spatial resolution vehicle emission inventory – Part 2

J. J. He et al.

Title Page

Abstract

Introduction

Conclusions

References

Tables

Figures

◀

▶

◀

▶

Back

Close

Full Screen / Esc

Printer-friendly Version

Interactive Discussion



Table 3. The rate of major species from vehicle emission in total emission (unit: %).

	CO	NO	NO ₂	HC	PM _{2.5}
CUACE ^a	29.8	32.1	30.4	80.0	23.4
CUACE ^b	31.1	35.5	33.6	49.0	25.3
HTSVE ^a	23.8	47.9	55.1	84.0	22.3
HTSVE ^b	21.3	46.6	53.9	55.8	20.6

^a and ^b represent July and December.

Development of a high temporal–spatial resolution vehicle emission inventory – Part 2

J. J. He et al.

Table 4. The contributions of traffic emission on ambient pollutant concentrations in Beijing.

Source	Period	Contribution (%)	Method
Hao et al. (2001)	1995	NO _x : 68.4; CO: 76.5	Numerical simulation based on ISCST3
Hao et al. (2005)	1999	NO _x : 74; PM ₁₀ : 14	Numerical simulation based on ISCST3
Zheng et al. (2005)	2000	PM _{2.5} : 6.7	Chemical mass balance receptor model (CMB)
Song et al. (2006)	2000	PM _{2.5} : 6.0–10.8	PCA/APCS and UNMIX
Cheng et al. (2007)	2002	PM ₁₀ : 28.7 ~ 42.9	MM5-APRS-CMAQ
Wang et al. (2008)	2001–2006	PM _{2.5} : 5.9; PM ₁₀ : 8.4	Positive matrix factorization (PMF)
Zhang et al. (2013)	2009–2010	PM _{2.5} : 4	PMF
Yu et al. (2013)	2010	PM _{2.5} : 17.1	PMF
S. W. Wu et al. (2014)	2010–2011	PM _{2.5} : 12.0	PMF and mixed-effects models
Cheng et al. (2013)	2011	PM _{2.5} : 22.5 ± 3.5; NO _x : 56–67	MM5-CMAQ and source apportionment methods
Liu et al. (2014)	2011	PM(NC): 47.9	PMF
Huang et al. (2014)	201 301	PM _{2.5} : 5.6	CMB and PMF

Title Page

Abstract

Introduction

Conclusions

References

Tables

Figures



Back

Close

Full Screen / Esc

Printer-friendly Version

Interactive Discussion

Development of a high temporal–spatial resolution vehicle emission inventory – Part 2

J. J. He et al.

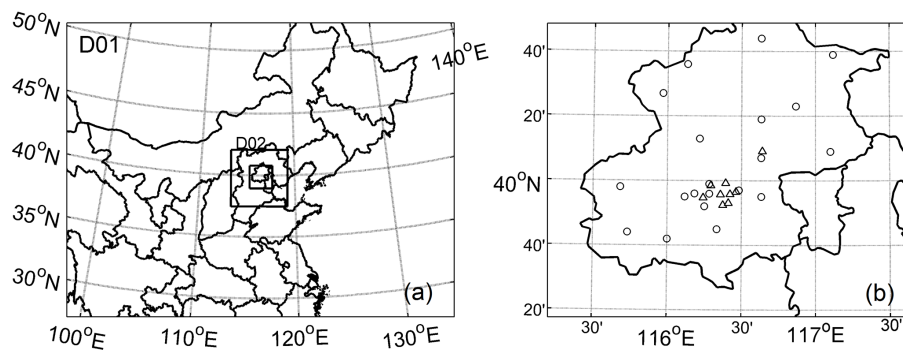


Figure 1. The model simulation domain **(a)** and observation station distribution (circle represents meteorological station, triangle represents environmental station) in inner domain **(b)**.

Title Page

Abstract

Introduction

Conclusions

References

Tables

Figures

◀

▶

◀

▶

Back

Close

Full Screen / Esc

Printer-friendly Version

Interactive Discussion

Development of a
high temporal–spatial
resolution vehicle
emission inventory –
Part 2

J. J. He et al.

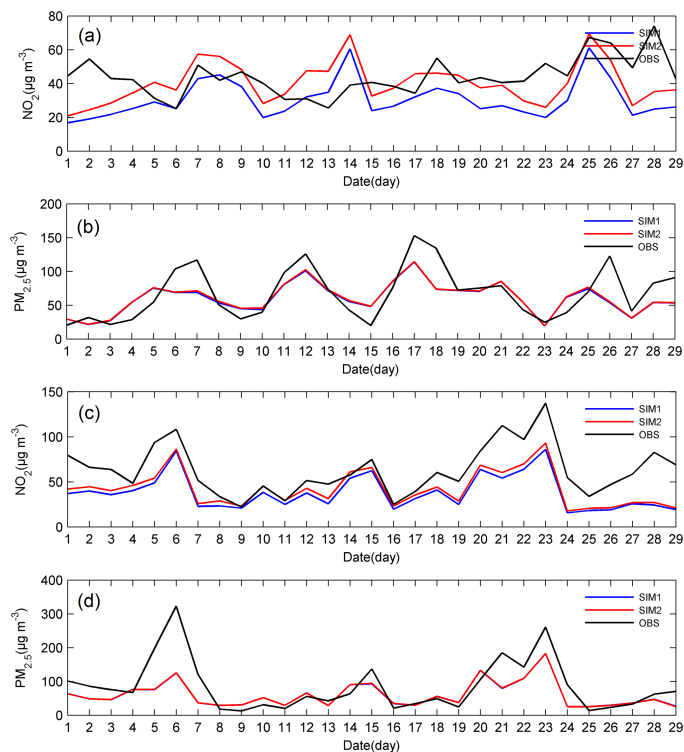


Figure 2. The comparison of site average NO_2 and $\text{PM}_{2.5}$ concentrations between SIM1, SIM2 and observation in July (a, b) and December (c, d) 2013.

Development of a
high temporal–spatial
resolution vehicle
emission inventory –
Part 2

J. J. He et al.

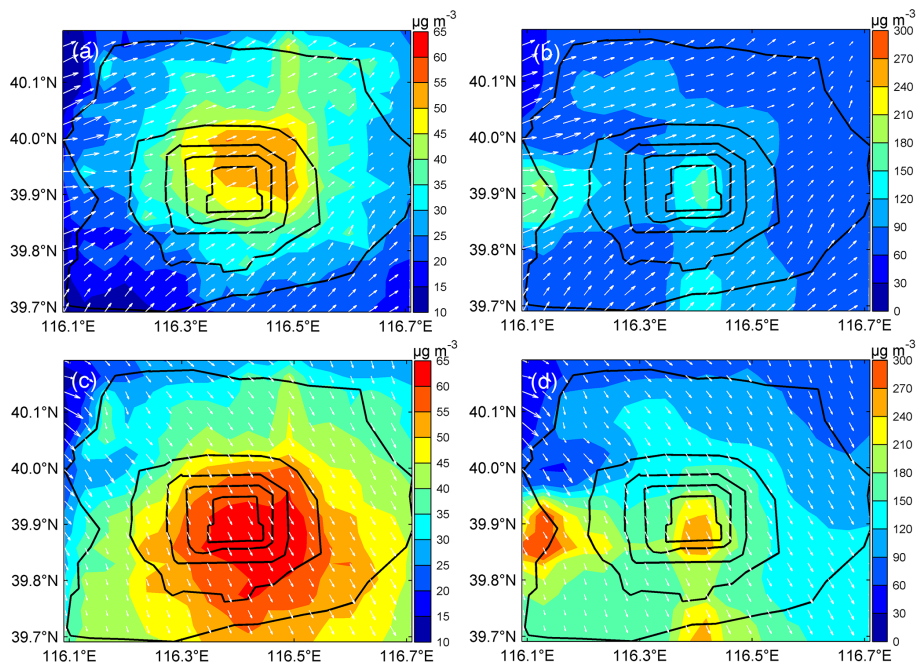


Figure 3. The spatial distribution of near-surface NO_2 and $\text{PM}_{2.5}$ mean concentration from SIM2 in July (a, b) and December (c, d) 2013 respectively. Black lines represent the main traffic arteries in Beijing, white arrows represent near-surface mean wind field.

Title Page

Abstract

Introduction

Conclusions

References

Tables

Figures

◀

▶

◀

▶

Back

Close

Full Screen / Esc

Printer-friendly Version

Interactive Discussion

Development of a high temporal–spatial resolution vehicle emission inventory – Part 2

J. J. He et al.

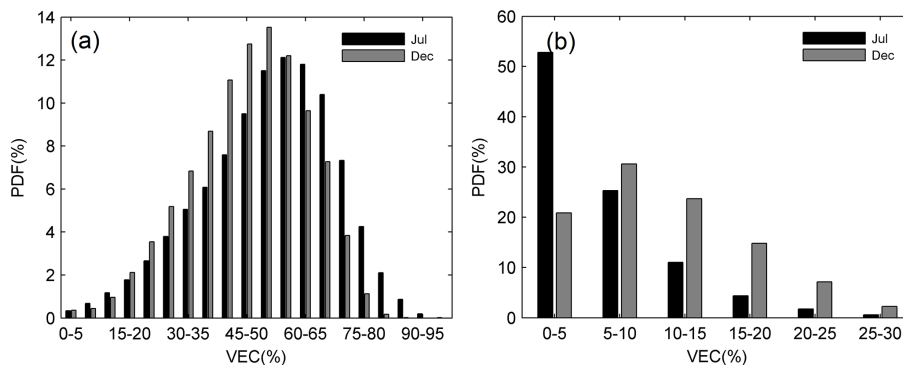


Figure 4. The probability density function (PDF) of instantaneous VEC for NO₂ (a) and PM_{2.5} (b).

Title Page

Abstract Introduction

Conclusions References

Tables Figures

◀ ▶

◀ ▶

Back Close

Full Screen / Esc

Printer-friendly Version

Interactive Discussion



Development of a
high temporal–spatial
resolution vehicle
emission inventory –
Part 2

J. J. He et al.

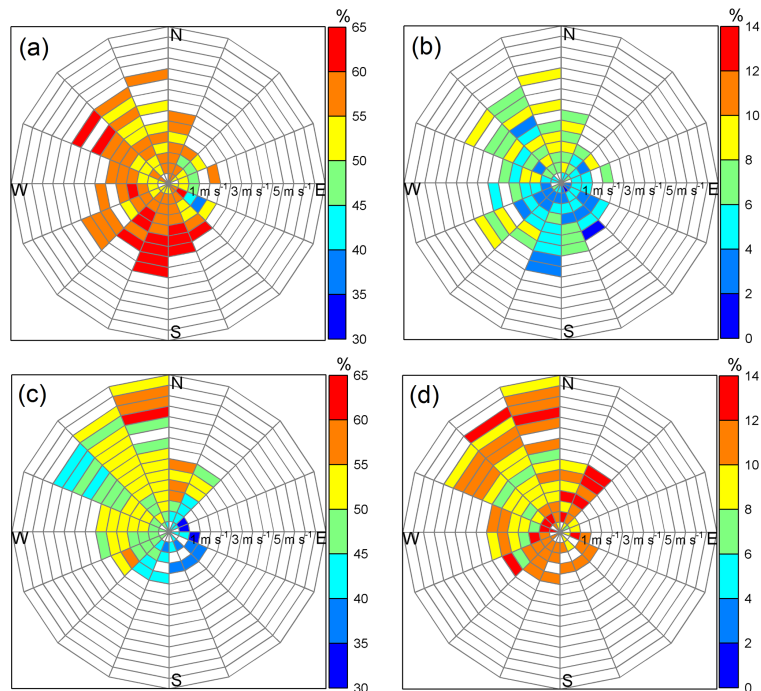


Figure 5. Wind dependency map of VEC to NO_2 and $\text{PM}_{2.5}$ in July (a, b) and December (c, d) 2013. Wind speeds are shown from 0 to 7.5 m s^{-1} .

[Title Page](#)[Abstract](#)[Introduction](#)[Conclusions](#)[References](#)[Tables](#)[Figures](#)[◀](#)[▶](#)[◀](#)[▶](#)[Back](#)[Close](#)[Full Screen / Esc](#)[Printer-friendly Version](#)[Interactive Discussion](#)

Development of a
high temporal–spatial
resolution vehicle
emission inventory –
Part 2

J. J. He et al.

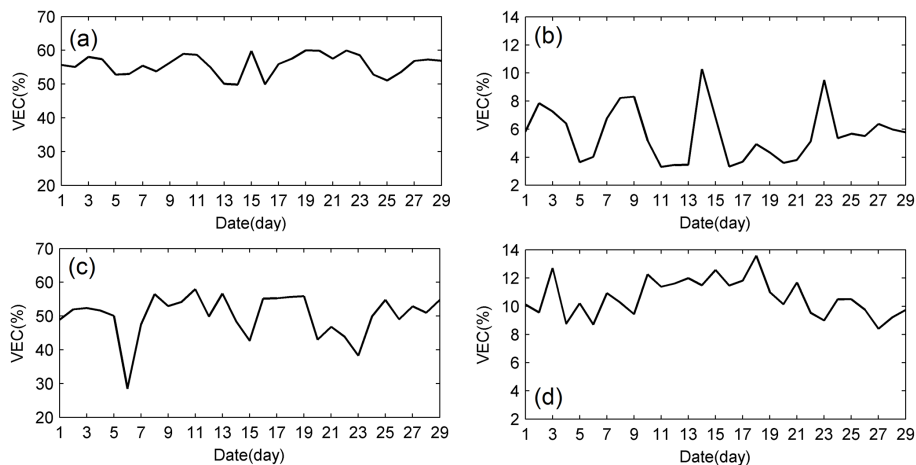


Figure 6. Time series of daily mean vehicle emission contribution rate on NO₂ and PM_{2.5} concentrations of Beijing main urban areas in July (a, b) and December (c, d) 2013.

[Title Page](#)[Abstract](#)[Introduction](#)[Conclusions](#)[References](#)[Tables](#)[Figures](#)[◀](#)[▶](#)[◀](#)[▶](#)[Back](#)[Close](#)[Full Screen / Esc](#)[Printer-friendly Version](#)[Interactive Discussion](#)

Development of a
high temporal–spatial
resolution vehicle
emission inventory –
Part 2

J. J. He et al.

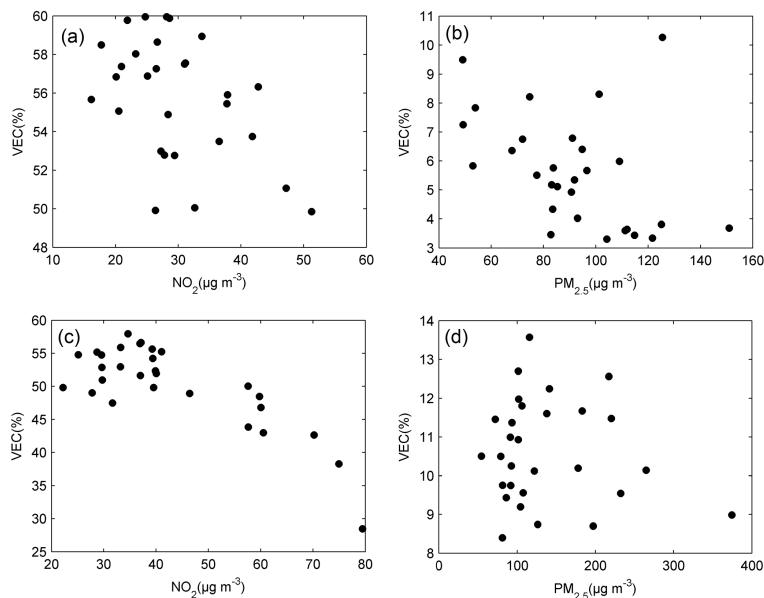


Figure 7. The scatter of daily mean concentration vs. VEC for NO_2 and $\text{PM}_{2.5}$ in July (**a, b**) and December (**c, d**).

[Title Page](#)[Abstract](#)[Introduction](#)[Conclusions](#)[References](#)[Tables](#)[Figures](#)[◀](#)[▶](#)[◀](#)[▶](#)[Back](#)[Close](#)[Full Screen / Esc](#)[Printer-friendly Version](#)[Interactive Discussion](#)

Development of a
high temporal–spatial
resolution vehicle
emission inventory –
Part 2

J. J. He et al.

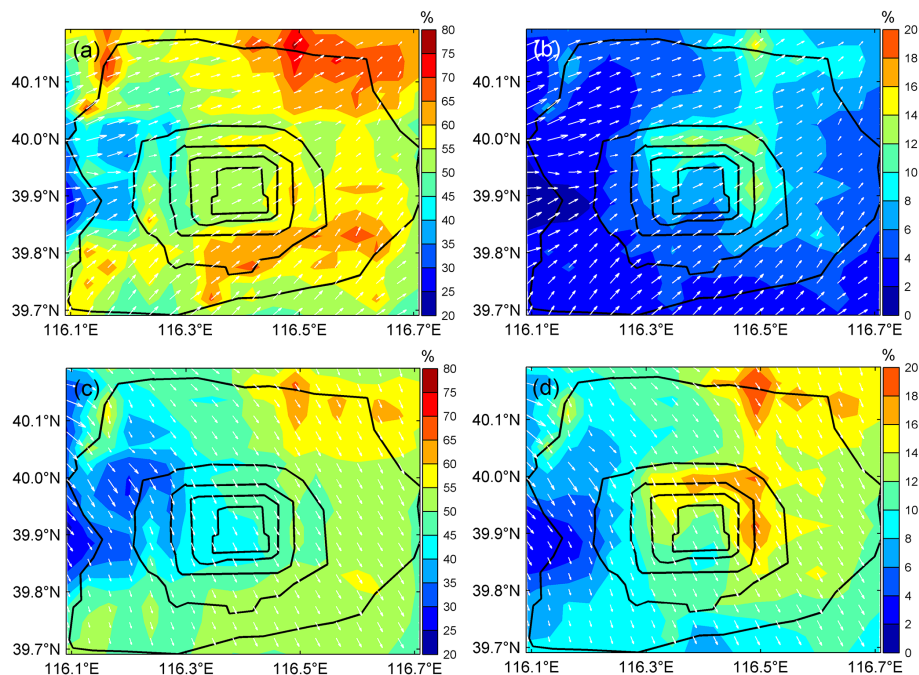


Figure 8. The spatial distribution of mean contribution rate of vehicle emission on NO_2 and $\text{PM}_{2.5}$ in July (**a, b**) and December (**c, d**) 2013. Black lines represent the main traffic arteries in Beijing, white arrows represent near-surface mean wind field.

Title Page

Abstract

Introduction

Conclusions

References

Tables

Figures

◀

▶

◀

▶

Back

Close

Full Screen / Esc

Printer-friendly Version

Interactive Discussion

Development of a
high temporal–spatial
resolution vehicle
emission inventory –
Part 2

J. J. He et al.

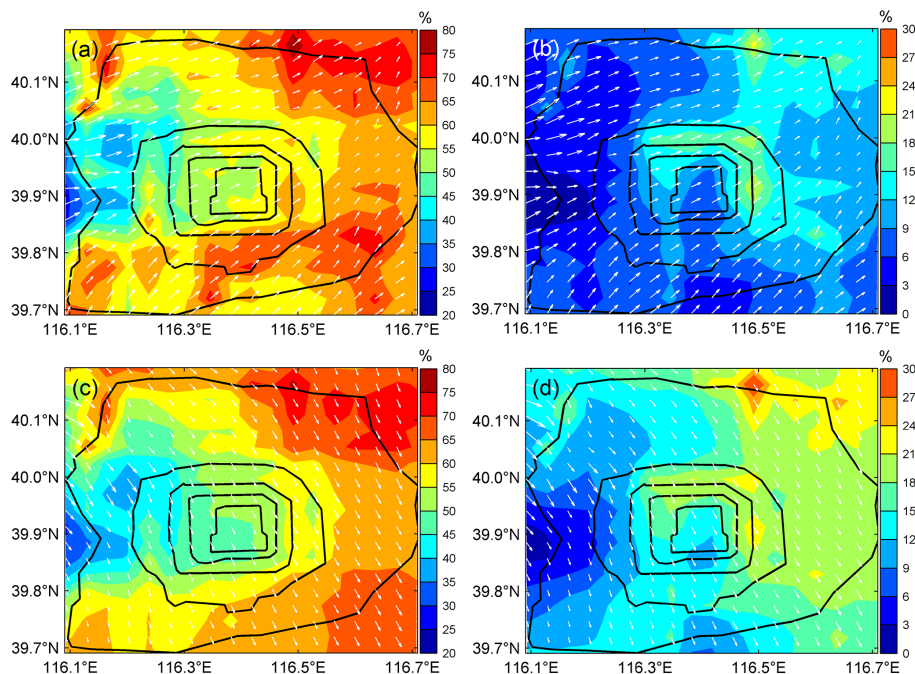


Figure 9. The spatial distribution of vehicle emission contribution in local emission to NO_2 and $\text{PM}_{2.5}$ in July (a, b) and December (c, d) 2013. Black lines represent the main traffic arteries in Beijing, white arrows represent near-surface mean wind field.

Title Page

Abstract

Introduction

Conclusions

References

Tables

Figures

◀

▶

◀

▶

Back

Close

Full Screen / Esc

Printer-friendly Version

Interactive Discussion